Learning Neural Light Transport

Paul Sanzenbacher
Autonomous Vision Group
University of Tübingen, Germany
paul.sanzenbacher@tue.mpg.de

Lars Mescheder
Amazon
Tübingen, Germany
lamesch@amazon.de

Andreas Geiger
Autonomous Vision Group
University of Tübingen, Germany
andreas.geiger@tue.mpg.de

Abstract

In this work, we investigate the importance of 3D reasoning for photorealistic and controllable neural rendering. Towards this goal, we develop an approach which explicitly formulates light transport in static and dynamic 3D scenes using a neural network. In contrast to existing approaches that operate primarily in the 2D image domain, our approach reasons in both 3D and 2D space, thus enabling both global illumination effects and manipulation of 3D scene geometry. Our differentiable model can be trained jointly on multiple scenes from noisy renderings and is able to produce photorealistic renderings with accurate lighting, capturing shadows, reflections and refractions. Moreover, it compares favorably to baselines which combine path tracing and image denoising at the same computational budget.

1. Introduction

Photorealistic rendering is a core problem in graphics and vision. Algorithms which are able to reason about direct and indirect illumination of a scene (i.e., global illumination) have become an essential building block for a wide range of applications such as gaming, virtual reality, movies and others. With the advent of deep learning, synthetic data generation emerged as another important application [2, 18, 77, 14, 85] with the potential to satisfy the notorious data hunger of modern deep learning systems. However, as modern deep neural networks require large amounts of data, most existing approaches rely on approximate rendering techniques to accelerate training [18, 77, 14, 85]. Training embodied agents (i.e., using reinforcement learning) poses even stronger demands wrt. simulation time [17].

Historically, photorealistic image synthesis is achieved using sampling-based rendering techniques [64, 86] where the physics of light transport [33] is exploited to transform a geometric description of a scene into a realistic image. However, while physically based rendering yields photorealistic results, it is also notoriously slow with rendering times of up to multiple hours for a single image. This makes it difficult to use in the context of training neural networks.

On the other hand, recent advances in deep generative models (e.g., GANs [22]) enabled the generation of highly realistic images [50, 34, 35] in milliseconds on commercial GPUs. However, most existing approaches make use of rather abstract latent representations which do not allow for precise control over the 3D content. Moreover, the lack of a holistic 3D scene description limits neural rendering approaches in their ability to render images that are consistent across viewpoints or time. While several recent works [78, 3, 52, 61, 53] have shown that neural networks can produce consistent images for a given scene, these approaches usually do not explicitly reason about light transport. Consequently, they are not able to handle fine-grained geometric scene manipulation and do not explicitly integrate illumination into the 3D representation. This motivates us to seek a more explicit neural representation that reasons about how light propagates through 3D space and that is able to capture dynamic global illumination effects. We summarize the contributions of this work as follows.

Contributions: We investigate the importance of 3D vs. 2D reasoning for efficient learning-based photorealistic rendering. Towards this goal, we present a learning-based approach (see Fig. 1 for a high-level overview) which allows for inferring photorealistic images from a point-cloud based scene representation in real time. In contrast to existing approaches, our method performs reasoning both in 3D and 2D space which allows for learning the physical light transport in a scene. This enables our method to handle scene modifications such as object translations, object removal and lighting changes. At the same time, our framework allows for learning useful heuristics (e.g., shadows that are not affected by moving objects) from the training data, enabling fast rendering without sacrificing quality. We introduce two variants of our approach: (1) a PointNet-based [66] model and (2) an extension of this model using photon sampling which improves the quality of shadows and specular reflections. We show, both theoretically and empirically, that our model can be trained without bias us-

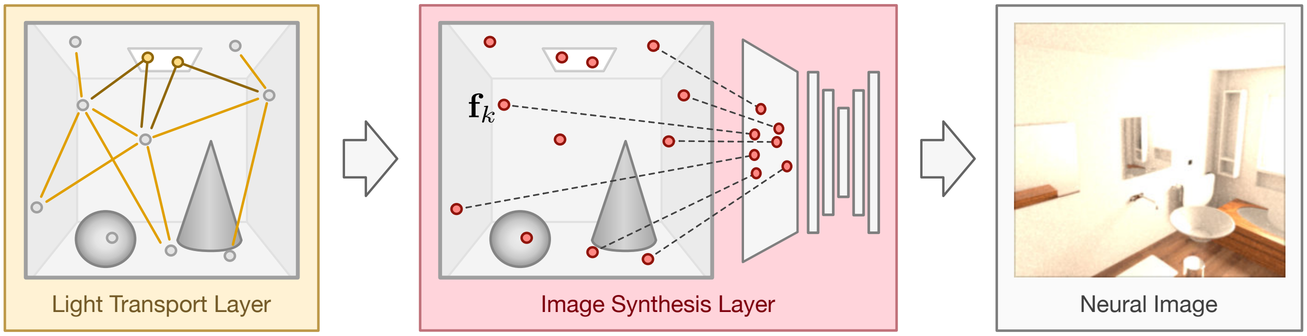

Figure 1. **Motivation.** We learn photorealistic rendering using a 3D Light Transport Layer in combination with a 2D Image Synthesis Layer. We demonstrate that our hybrid 3D-2D approach is able to synthesize realistic images with global illumination effects in real-time.

ing noisy renderings from a physically-based renderer. We will release our code and data upon publication.

2. Related Work

Rendering: Physically-based rendering (PBR) is a well-studied field [86, 64] where much of the research in recent years focuses on optimizing different parts of the rendering pipeline [54, 87, 70, 68] or denoising of noisy PBR renderings [7, 48, 8]. Moreover, there is a trend of making rendering algorithms differentiable in order to estimate scene properties [4, 47, 21, 20, 56, 31, 11] or to use them for training deep neural networks [84, 60, 43, 36]. While recent approaches strive to achieve real-time photorealistic rendering [75, 74], they often require additional assumptions such as temporal smoothness and are limited by temporal accumulation of information in screen space. In this paper, we probe the suitability of neural networks for learning light transport end-to-end, with the goal of differentiable rendering of dynamic scenes with complex lighting.

Generative Models: Recently, deep generative models such as variational autoencoders (VAEs) [26, 9, 38, 28] or (conditional) generative adversarial networks (GANs) [50, 34, 35, 6, 29] have demonstrated that neural networks are capable of generating photorealistic synthetic imagery. While some methods have addressed the problem of 3D controllable image synthesis [44, 57, 76, 58], these methods are currently restricted to a small number of comparably simple objects and do not explicitly reason about materials or global light transport.

Novel View Synthesis: Novel view synthesis approaches [63, 94, 15, 82, 16, 40, 12, 90, 91, 71, 10, 88, 16, 53, 92, 49, 72] focus on generating novel views of a single densely captured scene. However, since these methods lack an explicit scene representation which captures geometry, material and lighting, it is hard to gain precise control over their output. In contrast, we learn to render images in a differentiable manner from a *holistic* scene representation. Alhaija et al. [1] and Nalbach et al. [55] describe methods for generating renderings from multiple image buffers such as depth and materials. While this allows for rendering realistic images, a major limitation is that operations are performed in image space, making it hard to model global illumination.

Scene Representations: [3, 65, 52, 24] propose several deep models for rendering novel views from point clouds [19, 67, 93, 27]. However, existing approaches are limited to single objects or small static scenes. Moreover, they do not explicitly model light transport or consider only diffuse, homogeneous materials.

Recently, several alternative scene representations have been considered [79, 83, 51, 62, 59]. Sitzmann et al. [78] propose DeepVoxels, where a single static object-centric scene is encoded in a voxel grid of learned features. Rematas et al. [69] present Neural Voxel Renderer, a neural rendering framework that maps a voxelized scene to an RGB image. While both methods allow for rendering a sequence of coherent images, they are limited to comparably small scenes with a single object due to the high memory requirements of voxel-based representations. In contrast, our approach exploits a point-based scene representation and therefore scales to larger scenes with multiple objects. Furthermore, neither of them reasons explicitly about materials, light transport or global illumination.

Deferred Neural Rendering [83] proposes a neural texture representation for novel view synthesis of single objects with fixed lighting. Deep Appearance Models [45] encode the facial geometry and texture of a particular person. Neural Volumes [46] encode multiple images of an object into a neural volume representation which is rendered using ray marching. While producing impressive results, these works are trained for a single object or scene and assume static lighting. Moreover, they only allow for limited editing as their main focus is on view synthesis. In contrast, the focus of our work is on representing *multiple scenes* with a *single model*, where both objects and lighting can be dynamically rearranged in real time during inference.

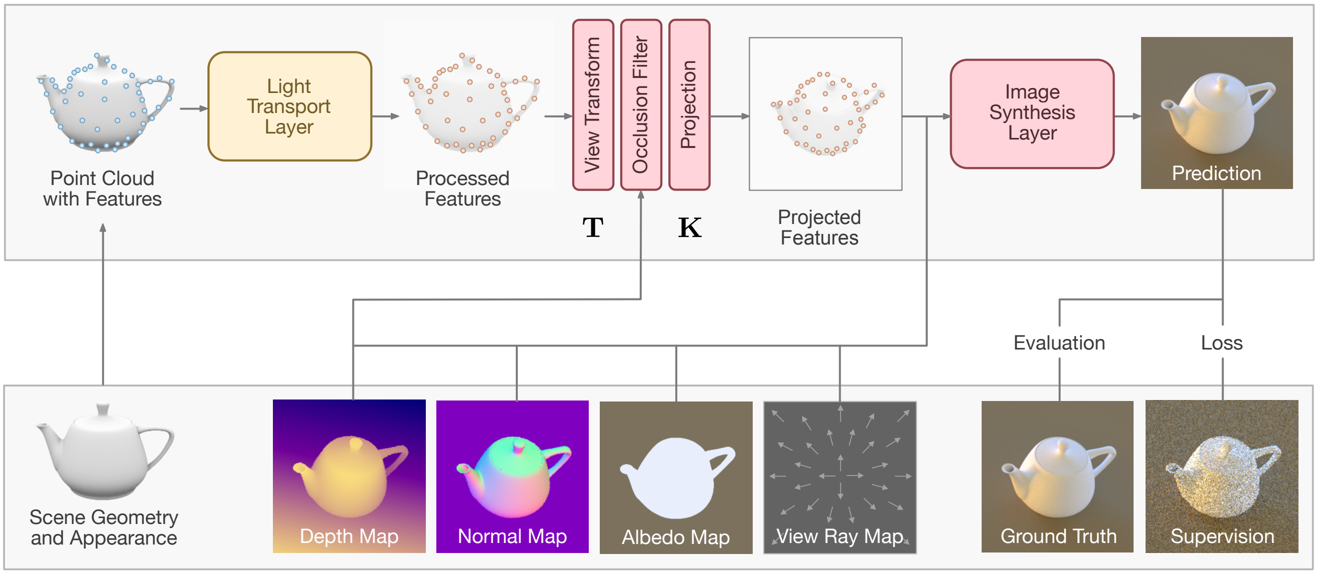

Figure 2. **Model Overview.** Given an input 3D mesh, we sample a uniform point cloud and associate each point with additional properties (albedo, emitted light color). These features are processed using the *Light Transport Layer* which learns to approximate the light transport in the scene. The resulting features are projected into the 2D image domain and occluded points are removed. The final image is synthesized using the *Image Synthesis Layer* that takes the projected features as well as additional low-level 2D image space information as input.

3. Method

Our goal is to train a deep neural network to render a photorealistic scene specified in terms of a 3D model in real time while accurately modeling light transport including reflection, refraction and global illumination. In this section, we first discuss our scene representation. Next, we describe our neural rendering architecture which is able to learn complex illumination effects by exploiting both 3D and 2D information. Finally, we describe how we train our model using noisy renderings for supervision and show that under moderate assumptions our gradient estimates are unbiased. An overview of our approach is given in Fig. 2.

Scene Representation: How should a 3D scene be represented for efficient and photorealistic rendering? Traditionally, 3D geometry is often represented in the form of textured 3D meshes. However, while meshes and texture atlases are compact and encode useful geometric properties, they are inconvenient for neural networks due to their irregular structures. In contrast, voxel-based representations can be processed conveniently using 3D convolutions, yet they are limited by their cubic memory requirements. In this work, we therefore opt for a hybrid 2D-3D representation consisting of both image-space buffers such as albedo, normal and depth maps as well as 3D information. We represent 3D information in form of an unstructured point cloud sampled from the scene's surface with learned feature embeddings enriched by albedo and light intensity/color.

Architecture: Our neural rendering model comprises three main parts as illustrated in Fig. 2: a Light Transport Layer, a 3D-to-2D projection step and an Image Synthesis Layer. The *Light Transport Layer* models global illumination effects that cannot be modeled in image space: consider for example a movable lamp which is present in the scene but not visible from the current point of view. While the position, color and intensity of the lamp strongly affect the overall illumination of the scene, a purely image-based method, by definition, will fail to reason about these effects. We therefore propose to reason in both 3D and 2D space.

Our Light Transport Layer takes a set of N_{surf} randomly sampled 3D surface points $\{\mathbf{p}_j\}$ and associated attributes for each point $\{\mathbf{a}_j\}$ as input. These attributes comprise the surface albedo and the light intensity/color emitted by the point if the point is located on a light-emitting surface. Our goal is to define an architecture that is able to model or approximate light transport in a scene sufficiently well such that illumination effects like reflections and shadows are predicted correctly.

Towards this goal, we first predict a feature embedding $\mathbf{f}_j$ for each point $\mathbf{p}_j$ using a PointNet-based architecture [66]. While we found that such a global representation is able to reason about global illumination to some extent, we additionally propose a more explicit model for light transport to model illumination effects more accurately. Inspired by *photon mapping* [32], we sample additional N_{phot} photon points $\{\mathbf{q}_k\}$ from all light sources in the scene. Photons are randomly cast into the scene and their (first) intersection with the scene geometry $\{\mathbf{q}'_k\}$ is computed. For each

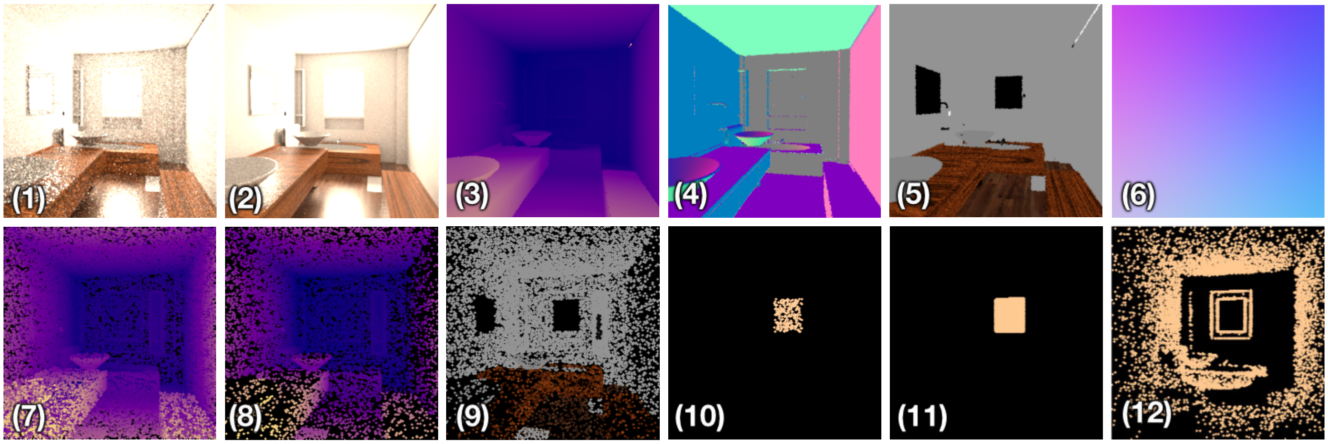

Figure 3. **Visualization of a Single Data Sample.** (1) Noisy supervision (used during training). (2) Ground truth rendering (for reference only, not used during training). (3-6) Image-space information $\mathbf{A}$: depth, normal, albedo and view ray maps. (7) Point cloud $\{\mathbf{p}_j\}$. (8) Point cloud $\{\mathbf{p}_j\}$ after occlusion masking. (9) Per-point albedo which serves as an input to the light transport layer. (10) Emitting surface points $\{\mathbf{q}_j\}$ colored in emitter spectrum. (11) Emitting photon points $\{\mathbf{q}_k\}$. (12) Intersections of emitted photons with scene $\{\mathbf{q}'_k\}$.

photon intersection $\mathbf{q}'_k$ we process the position, color and direction of the initial photon point $\mathbf{q}_k$ with a fully connected neural network, resulting in a feature vector $\mathbf{f}_k$ at $\mathbf{q}'_k$. The photon network thus encodes information about the light color, intensity and direction which is necessary for photorealistic shading.

Next, we remove occluded points in the 3D scene using the depth map $\mathbf{D}$ and project the remaining point features $\mathbf{f}_j$ and photon features $\mathbf{f}_k$ onto the image plane using perspective projection $\phi(j) = [\mathbf{K}\mathbf{T}\mathbf{p}_j]$ where $\mathbf{p}_j$ denotes the point location, $\mathbf{K}$ is the camera matrix and $\mathbf{T}$ the rigid world-to-view transformation matrix. The resulting 2D feature map $\mathbf{F}$ is obtained by pooling the features of all points projecting onto the same pixel. Formally, we obtain $\mathbf{F}_\mathbf{u}$ at pixel $\mathbf{u}$ as

$$\mathbf{F}_\mathbf{u} = \begin{cases} \frac{1}{|\phi^{-1}(\mathbf{u})|} \sum_{j \in \phi^{-1}(\mathbf{u})} \mathbf{f}_j & \text{if } \phi^{-1}(\mathbf{u}) \neq \emptyset \\ 0, & \text{otherwise} \end{cases} \tag{1}$$

where $\phi^{-1}(\mathbf{u}) := \{j : \phi(j) = \mathbf{u}\}$ denotes the inverse projection. We concatenate the resulting feature map $\mathbf{F}$ with additional image-space information $\mathbf{A}$ (i.e., a depth map, a normal map and an albedo map) which we obtain using OpenGL shaders. Note that this additional image-space information can be computed cheaply and complements the global scene representation $\mathbf{F}$ with high-frequency albedo, normal and depth information. Additionally, we create a view ray map that encodes for each pixel a normalized vector pointing from the camera center to the pixel center in world coordinates. This information is necessary for learning specular reflection and refraction effects. The final image synthesis is performed using the *Image Synthesis Layer* which we implement using a conventional 2D U-Net architecture [73]. Fig. 3 provides an illustration of the various inputs and features for a bathroom scene.

Training: We train our model using a dataset $\mathcal{D} = \{(\mathbf{X}_i, \hat{\mathbf{I}}_i)\}_{i=1}^N$ which comprises pairs of 3D scene representations $\mathbf{X}_i$ and cheap noisy renderings $\hat{\mathbf{I}}_i$ that are obtained from a physically-based renderer which we run for few iterations. The input $\mathbf{X}_i = (\mathbf{P}_i, \mathbf{T}_i, \mathbf{A}_i)$ consists of a scene represented by a point cloud $\mathbf{P}_i$, a view represented by a world-to-view transform $\mathbf{T}_i$ and additional image-space information $\mathbf{A}_i$. Let $\varphi_\theta(\cdot)$ denote our model with θ the parameters of the light transport and image synthesis layer. Our objective is to find a parameter vector θ^* which minimizes the mean squared error (MSE) between the image predicted by our model $\varphi_\theta(\mathbf{X}_i)$ and the noisy rendering $\hat{\mathbf{I}}_i$:

$$\theta^* = \arg\min_\theta \sum_{i=1}^N \|\hat{\mathbf{I}}_i - \varphi_\theta(\mathbf{X}_i)\|^2 \tag{2}$$

Since obtaining clean renderings is very time-consuming, we propose the use of noisy renderings from a physically-based renderer [42, 39]. One of our key insights and contributions is to demonstrate that we can exploit the unbiasedness of rendering algorithms like bidirectional path tracing [41] to obtain unbiased gradient estimates:

Lemma 1. *Let $\mathbf{X}$ be an input representation of a scene, φ_θ our rendering network and $\hat{\mathbf{I}}$ a noisy rendering of $\mathbf{X}$ following a distribution $p(\hat{\mathbf{I}}|\mathbf{X})$ which depends on the chosen sampling-based rendering algorithm. Assume that the true (noise-free) rendering is given by $\mathbf{I}(\mathbf{X})$. Further assume that the rendering algorithm is unbiased, i.e., $\mathbb{E}_{\hat{\mathbf{I}}|\mathbf{X}}[\hat{\mathbf{I}}] = \mathbf{I}(\mathbf{X})$. In this case, the following equality holds, i.e., the gradient estimates are also unbiased:*

$$\mathbb{E}_{\hat{\mathbf{I}}|\mathbf{X}}\left[\nabla_\theta \|\varphi_\theta(\mathbf{X}) - \hat{\mathbf{I}}\|^2\right] = \nabla_\theta \|\varphi_\theta(\mathbf{X}) - \mathbf{I}(\mathbf{X})\|^2 \tag{3}$$

Proof. See supplementary material. □

Implementation Details: For the Light Transport Layer, we use a PointNet-based architecture [66] with ResNet-blocks [23] of depth two. For the Image Synthesis Layer we use a UNet [73] with four downsampling and four upsampling blocks. The network architecture used for photon feature creation is a fully-connected ResNet [23] architecture with two residual blocks consisting of two fully-connected layers each. The input, hidden and output dimension is the same as for the PointNet architecture. For training, we use the Adam optimizer [37] with a learning rate of $5 \cdot 10^{-4}$ and a batch size of 128 for static scenes and 32 for dynamic scenes (see Section 4). The learning rate is decayed exponentially by multiplying it by a factor of 0.99 after every epoch. More details are provided in the supplementary.

4. Experiments

In our experiments, we investigate the importance of 3D reasoning for learning photorealistic rendering from noisy observations. We conduct two types of experiments: In our first set of experiments, we analyze the importance of 3D information and the influence of the different components of the Image Synthesis Layer. To analyze these properties independently of light transport, we first run our approach on a **static scene** observed from varying viewpoints. Our second set of experiments addresses **dynamic scenes** (moving objects and light sources) using our complete pipeline including the Light Transport Layer.

Datasets: For our experiments on static scenes, we evaluate our approach on a simple static indoor scene containing a table, two light sources and a glass egg [86]. Our experiments on dynamic scenes are based on four realistic indoor scenes from [5]. We use *Mitsuba* [30] for both rendering and point sampling. Renderings are created using bidirectional path tracing, a modification of path tracing that is unbiased and converges faster [86]. For each scene, we create a training set of 100,000 images at a resolution of 256×256 pixels, varying the camera pose for each training sample. We sample 10,000 surface points for each scene. For our experiments on dynamic scenes, we randomly translate or remove objects in addition to varying the camera pose.

Baselines: For our main experiment on dynamic scenes we use three baseline methods: (1) a 2D CNN baseline which predicts images from the image-space input $\mathbf{A}_i$ alone, (2) a simple denoising approach similar to the model of Lehtinen et al. [42], which learns to predict smooth renderings using noisy renderings as input and (3) a simple feature projection approach similar to Aliev et al. [3] without Light Transport Layer. For the denoising approach we trade off accuracy with run-time by adapting the number of pixels for which we run the bidirectional path tracer. We report results for $1/1$, $1/4$, $1/16$ and $1/64$ of the total number of image pixels with four samples per pixel, setting all other pixels to black. For fair comparison, we use the *same* light-weight 2D convolutional architecture for all baselines and our image synthesis layer. We remark that the primary focus of our experiments is not on improving the state-of-the-art in image denoising, but to demonstrate the efficacy of joint 2D and 3D reasoning for learning-based neural rendering. Both, our model as well as the denoising baselines, would benefit from more powerful (but slower) backbones.

Metrics: For quantitative comparison, we evaluate mean squared error (MSE) and mean structural similarity index (MSSIM) [89] with a window size of 7×7 pixels. MSE and MSSIM measure mostly low-level similarity. To also measure perceptual similarity, we compute the FID [25] and a Feature-L1 distance [62] between predicted and ground truth images. For both the FID and Feature-L1 distance, we use the features of the final average pooling layer of an Inception v3 network [80, 81] trained on ImageNet [13].

4.1. Ablation Study on Static Scene

For our ablation study, we first conduct experiments on a single static scene that does not contain moving objects or light sources. Our primary goal is to investigate the influence of the different elements of the Image Synthesis Layer as well as the importance of 3D information.

We compare the performance of our model without Light Transport Layer for different input modalities. Fig. 4 shows the different configurations which are evaluated against each other. We choose a subset of 6 (out of $2^4 = 16$) representative configurations to highlight the importance of each input. While configuration 1, 2 and 3 use only 3D information (but no image space information), configuration 4 and 5 rely solely on image space information. Finally, configuration 6 combines both 3D and image space information.

Results: Configurations 1, 2, 3 and 5 show similar performance in terms of MSE, while configuration 5, which does not receive any projected point cloud information as input, clearly outperforms the other three configurations in terms of MSSIM and Fréchet inception distance (FID). However, surface normal information only yields good results if supplemented by viewpoint information, as becomes evident when comparing configurations 4 and 5. The most important insight is that all inputs in combination (configuration 6), outperform the other configurations for all metrics by a large margin. This result supports our initial hypothesis that reasoning in both 3D and 2D is crucial for this task. Fig. 4 (top) shows qualitative results. While configurations 1, 2 and 3 achieve reasonable qualitative results, they also contain several artifacts (e.g., the table) which do not occur in configuration 6. Configurations 4 and 5 do not exploit 3D information, thus severely degrading visual fidelity. This highlights the importance of 3D information for learning-based rendering. Configuration 6 which uses both 2D as

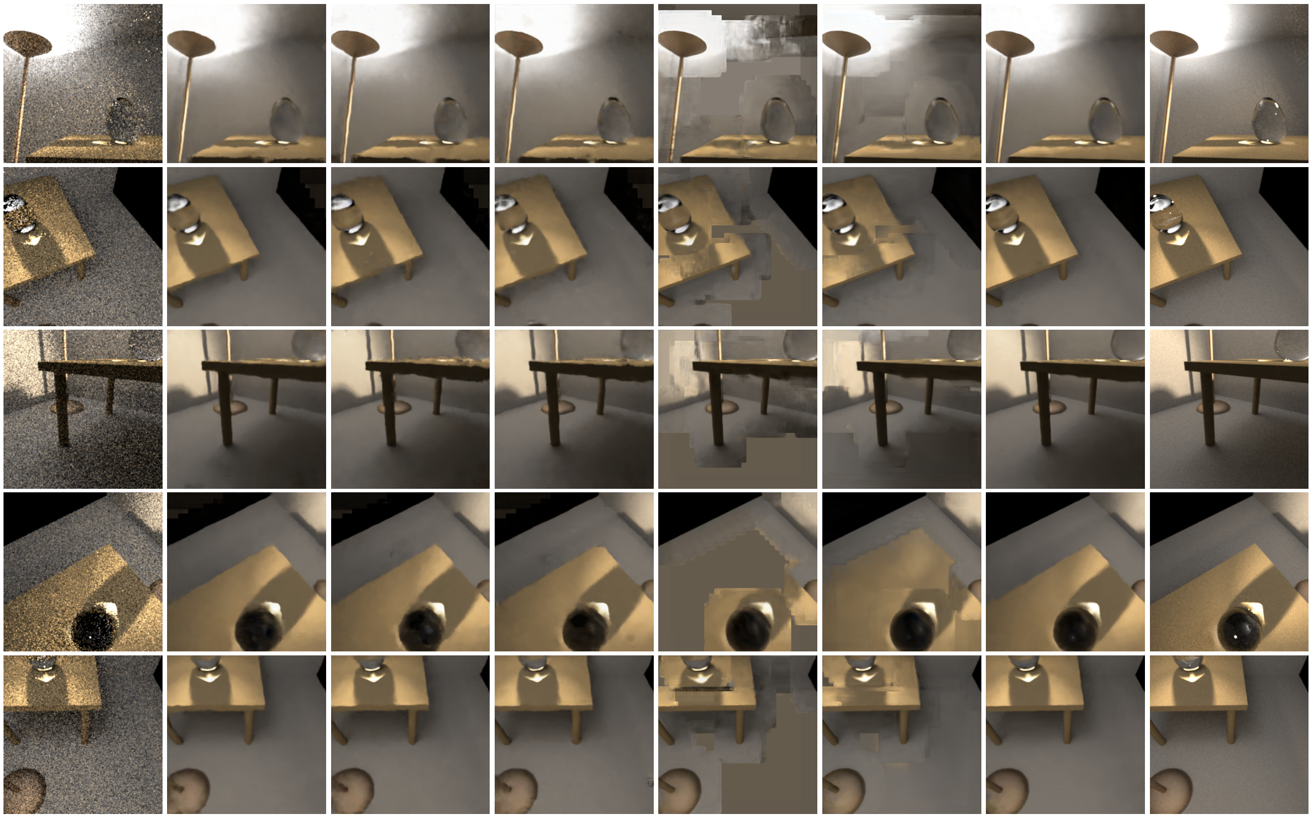

config	position	point features	normal map	ray direction map	MSE	MSSIM	FID
1	yes	no	no	no	0.0106	0.81	154.6
2	no	yes	no	no	0.0107	0.80	158.6
3	yes	yes	no	no	0.0108	0.81	149.4
4	no	no	yes	no	0.0161	0.78	138.1
5	no	no	yes	yes	0.0107	0.83	124.0
6	yes	yes	yes	yes	**0.0084**	**0.88**	**86.1**

Figure 4. **Ablation Study on Static Scene.** Comparing different input configurations for a static scene. The metrics are evaluated on a separate held-out validation set comprising 2048 samples. All networks were trained for 200,000 iterations with a batch size of 128. Note how the full model (6) is able to predict images that are significantly less noisy than the supervision signal used for training.

well as 3D information yields the best results. Moreover, it is remarkable that our model predicts images that are significantly less noisy than the images used for training.

4.2. Results on Dynamic Scenes

To investigate the utility of 3D reasoning, we now turn our attention to dynamic scenes where objects (and light sources) are modified.

4.2.1 Dynamic Objects and Fixed Lights

We first train our network on a set of four scenes where objects are randomly removed or translated in the scene, but keep all light sources fixed.

Results: Fig. 5 shows qualitative and quantitative results for our approach and the baselines. We clearly see that our full model which uses both the Light Transport and the Image Synthesis Layers outperforms the other real-time approaches (lower section of the table), both qualitatively and quantitatively in terms of MSE, MSSIM, FID and Feature-L1 distance. While the non-real-time denoising approach "Denoising (1/1)" achieves the best results, the real-time denoising approach that uses much fewer samples performs the worst. We further analyze this behavior by plotting the MSSIM as a function of rendering time in Fig. 6. While denoising approaches are able to achieve compelling results, the proposed neural rendering approach provides a better accuracy/runtime trade-off while being fully differentiable.

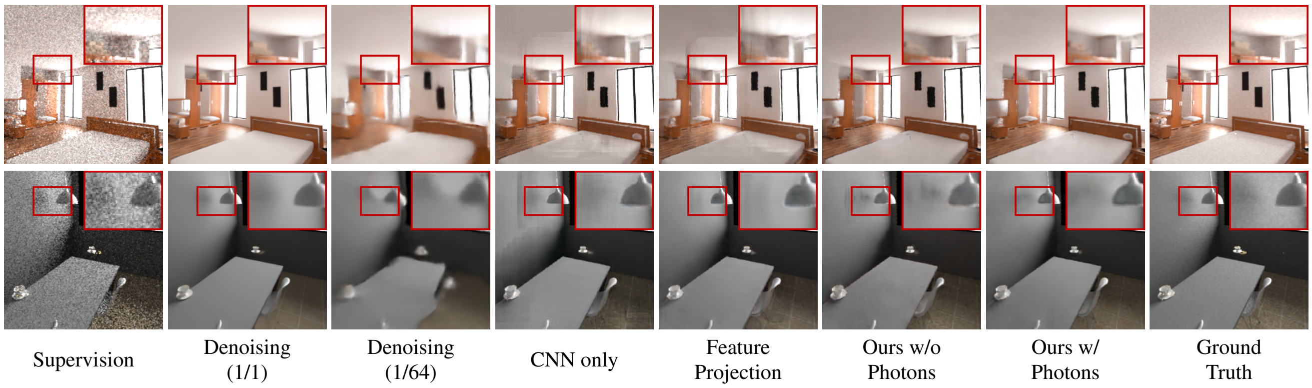

Architecture	time / frame	MSE (↓)	MSSIM (↑)	FID (↓)	Feature L1 (↓)
Denoising (1/1)	1.5059s	0.0005	0.880	26.4	0.163
Denoising (1/64)	0.0283s	0.0029	0.781	94.0	0.281
CNN only	0.0191s	0.0043	0.835	36.1	0.195
Feature Projection	0.0210s	0.0037	0.841	32.5	0.185
Ours (w/o Photons)	0.0243s	0.0044	0.841	31.4	0.184
Ours (w/ Photons)	0.0459s	**0.0028**	**0.849**	**30.6**	**0.182**

Figure 5. **Dynamic Objects and Fixed Lights.** Results on dynamic scenes where objects are modified but light sources kept fixed. We show the non-real-time denoising baseline "Denoising (1/1)" for reference. Additional results are provided in the supplementary material.

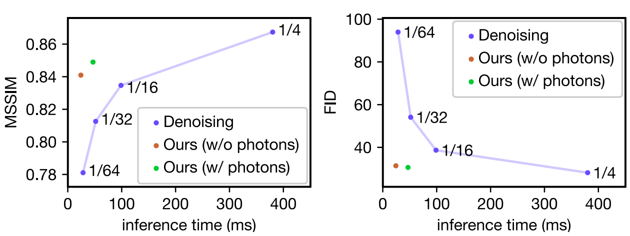

Figure 6. **Dynamic Objects and Fixed Lights.** Quantitative comparison of our approach to the denoising baseline, varying the sample density. Reconstruction accuracy in terms of MSSIM and FID over inference time. Numbers refer to the ratio of dropped pixels.

As evident from Fig. 5, our simple feature projection baseline performs only slightly weaker than our variant without photon mapping. We attribute this to the fact that most of the light field in the scene can be encoded in local features and only dynamic parts like sharp shadows have to be learned. This highlights the capability of neural rendering approaches to learn useful heuristics from the training data. As in the previous experiment, our full architecture with photon mapping (which reasons more explicitly about light transport) achieves the best quantitative results.

4.2.2 Dynamic Objects and Dynamic Lights

In the previous experiment, both the feature projection and our approach without photons were able to handle shadows and other illumination effects well. The reason for this is that the light sources were assumed static, making it possible to encode viewpoint-dependent light properties into the point features. However, by design the feature projection baseline is unable to acquire an understanding of illumination effects in the presence of movable light sources that are not present in the current view. To see this effect, we augment the dataset from the previous experiment by turning all static light sources off and replacing them with a rectangular area light at the ceiling, which we move randomly.

Results: Results from our method with photons, our approach without photons and the feature projection baseline are shown in Fig. 7. We observe that the feature projection baseline produces considerable artifacts while our approach with photons leads to much sharper shadows and more consistent global illumination. This is also evident from the error maps in Fig. 7. The last row shows a failure case of our approach which does not accurately recover the mirror reflection due to the limited number of samples. We provide a full quantitative evaluation in the supplementary material.

5. Conclusion

In this work, we conducted a systematic investigation of the importance of 3D vs. 2D reasoning for learning-based photorealistic neural rendering. Our experiments demonstrated that neural rendering benefits from joint 3D-2D reasoning. This also confirms our initial hypothesis that reasoning in 3D is indeed helpful in the presence of moving objects and light sources. In contrast to denoising methods which rely on outputs from a sampling-based renderer, the presented approach is fully differentiable and can be used for training deep models using differentiable rendering while faithfully capturing global illumination effects.

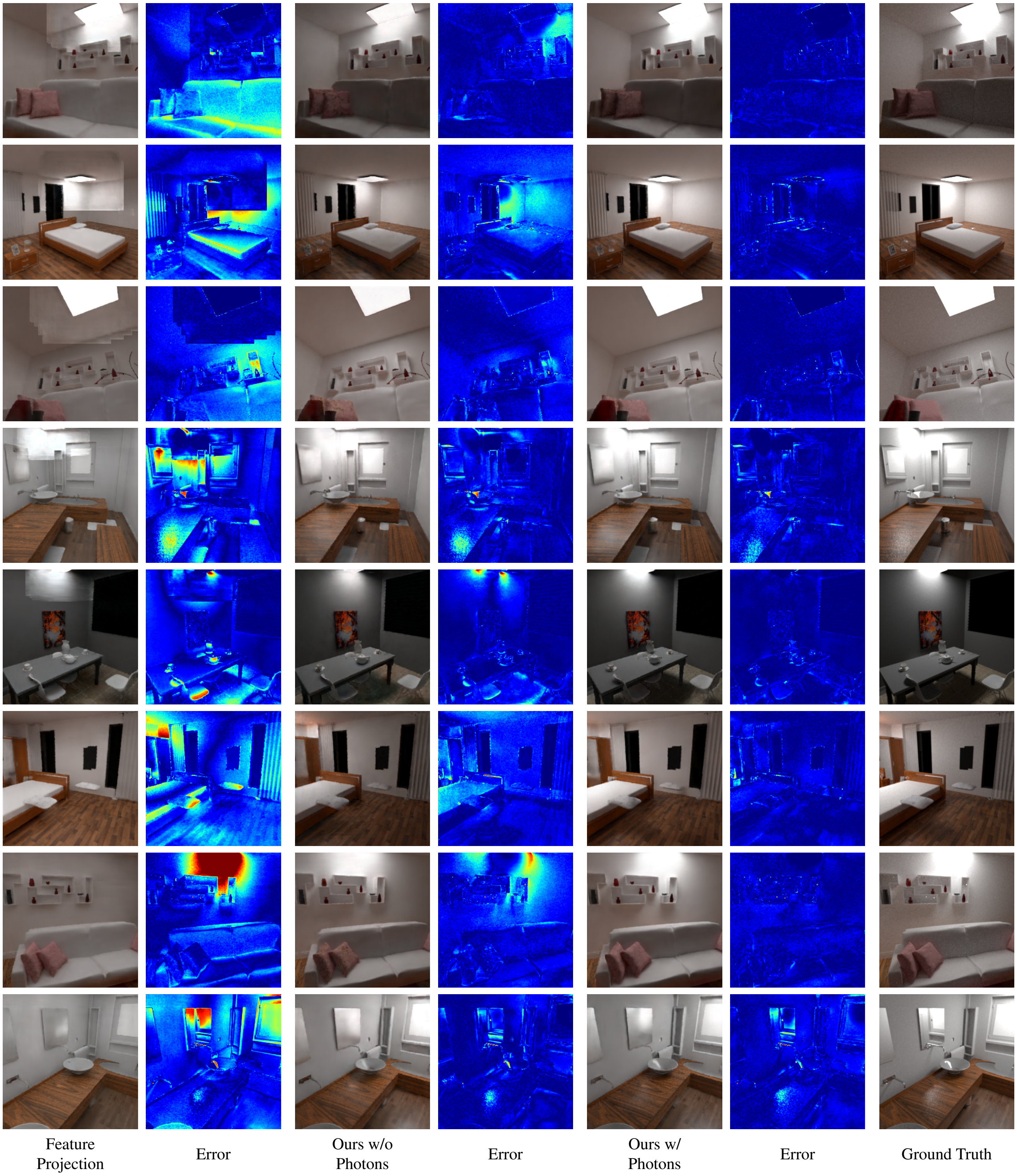

Figure 7. **Dynamic Objects and Dynamic Lights.** We show the output of the feature projection baseline and our network's predictions with and without photons alongside the corresponding error maps for moving light sources. The last row shows a failure case of our approach which in this case is not able to accurately recover the mirror reflection due to the limited number of reflected samples.

References

[1] Hassan Alhaija, Siva Mustikovela, Andreas Geiger, and Carsten Rother. Geometric image synthesis. In *Proc. of the Asian Conf. on Computer Vision (ACCV)*, 2018. 2

[2] Hassan Alhaija, Siva Mustikovela, Lars Mescheder, Andreas Geiger, and Carsten Rother. Augmented reality meets computer vision: Efficient data generation for urban driving scenes. *International Journal of Computer Vision (IJCV)*, 126(9):961–972, 2018. 1

[3] Kara-Ali Aliev, Dmitry Ulyanov, and Victor S. Lempitsky. Neural point-based graphics. *arXiv.org*, 1906.08240, 2019. 1, 2, 5

[4] Dejan Azinović, Tzu-Mao Li, Anton Kaplanyan, and Matthias Nießner. Inverse path tracing for joint material and lighting estimation. In *Proc. Computer Vision and Pattern Recognition (CVPR), IEEE*, 2019. 2

[5] Benedikt Bitterli. Rendering resources, 2016. https://benedikt-bitterli.me/resources/. 5

[6] Andrew Brock, Jeff Donahue, and Karen Simonyan. Large scale GAN training for high fidelity natural image synthesis. In *Proc. of the International Conf. on Learning Representations (ICLR)*, 2019. 2

[7] A. Buades, B. Coll, and J. . Morel. A non-local algorithm for image denoising. In *Proc. IEEE Conf. on Computer Vision and Pattern Recognition (CVPR)*, 2005. 2

[8] Chakravarty R. Alla Chaitanya, Anton S. Kaplanyan, Christoph Schied, Marco Salvi, Aaron E. Lefohn, Derek Nowrouzezahrai, and Timo Aila. Interactive reconstruction of monte carlo image sequences using a recurrent denoising autoencoder. *ACM Trans. on Graphics*, 36(4):98:1–98:12, 2017. 2

[9] Tony F. Chan and Jianhong Shen. Variational image inpainting. 58:579–619, 2005. 2

[10] Qifeng Chen and Vladlen Koltun. Photographic image synthesis with cascaded refinement networks. In *Proc. of the IEEE International Conf. on Computer Vision (ICCV)*, 2017. 2

[11] Wenzheng Chen, Huan Ling, Jun Gao, Edward Smith, Jaako Lehtinen, Alec Jacobson, and Sanja Fidler. Learning to predict 3d objects with an interpolation-based differentiable renderer. In *Advances in Neural Information Processing Systems (NIPS)*, 2019. 2

[12] Xi Chen, Xi Chen, Yan Duan, Rein Houthooft, John Schulman, Ilya Sutskever, and Pieter Abbeel. Infogan: Interpretable representation learning by information maximizing generative adversarial nets. In *Advances in Neural Information Processing Systems (NIPS)*, 2016. 2

[13] Jia Deng, Wei Dong, Richard Socher, Li jia Li, Kai Li, and Li Fei-fei. Imagenet: A large-scale hierarchical image database. In *Proc. IEEE Conf. on Computer Vision and Pattern Recognition (CVPR)*, 2009. 5

[14] Alexey Dosovitskiy, German Ros, Felipe Codevilla, Antonio Lopez, and Vladlen Koltun. CARLA: An open urban driving simulator. In *Proc. Conf. on Robot Learning (CoRL)*, 2017. 1

[15] Alexey Dosovitskiy, Jost Tobias Springenberg, and Thomas Brox. Learning to generate chairs with convolutional neural networks. In *Proc. IEEE Conf. on Computer Vision and Pattern Recognition (CVPR)*, 2015. 2

[16] S. M. Ali Eslami, Danilo Jimenez Rezende, Frédéric Besse, Fabio Viola, Ari S. Morcos, Marta Garnelo, Avraham Ruderman, Andrei A. Rusu, Ivo Danihelka, Karol Gregor, David P. Reichert, Lars Buesing, Theophane Weber, Oriol Vinyals, Dan Rosenbaum, Neil C. Rabinowitz, Helen King, Chloe Hillier, Matt M. Botvinick, Daan Wierstra, Koray Kavukcuoglu, and Demis Hassabis. Neural scene representation and rendering. *Science*, 360:1204–1210, 2018. 2

[17] Lasse Espeholt, Hubert Soyer, Rémi Munos, Karen Simonyan, Volodymyr Mnih, Tom Ward, Yotam Doron, Vlad Firoiu, Tim Harley, Iain Dunning, Shane Legg, and Koray Kavukcuoglu. IMPALA: scalable distributed deep-rl with importance weighted actor-learner architectures. In Jennifer G. Dy and Andreas Krause, editors, *Proc. of the International Conf. on Machine learning (ICML)*, 2018. 1

[18] Adrien Gaidon, Qiao Wang, Yohann Cabon, and Eleonora Vig. Virtual worlds as proxy for multi-object tracking analysis. In *Proc. IEEE Conf. on Computer Vision and Pattern Recognition (CVPR)*, 2016. 1

[19] Alberto Garcia-Garcia, Francisco Gomez-Donoso, José García Rodríguez, Sergio Orts-Escolano, Miguel Cazorla, and Jorge Azorín López. Pointnet: A 3d convolutional neural network for real-time object class recognition. In *International Joint Conference on Neural Networks (IJCNN)*, 2016. 2

[20] Ioannis Gkioulekas, Anat Levin, and Todd E. Zickler. An evaluation of computational imaging techniques for heterogeneous inverse scattering. In *Proc. of the European Conf. on Computer Vision (ECCV)*, 2016. 2

[21] Ioannis Gkioulekas, Shuang Zhao, Kavita Bala, Todd E. Zickler, and Anat Levin. Inverse volume rendering with material dictionaries. *ACM Trans. on Graphics*, 2013. 2

[22] Ian J. Goodfellow, Jean Pouget-Abadie, Mehdi Mirza, Bing Xu, David Warde-Farley, Sherjil Ozair, Aaron C. Courville, and Yoshua Bengio. Generative adversarial nets. In *Advances in Neural Information Processing Systems (NIPS)*, 2014. 1

[23] Kaiming He, Xiangyu Zhang, Shaoqing Ren, and Jian Sun. Deep residual learning for image recognition. In *Proc. IEEE Conf. on Computer Vision and Pattern Recognition (CVPR)*, 2016. 5

[24] P. Hermosilla, S. Maisch, T. Ritschel, and T. Ropinski. Deep-learning the latent space of light transport. *Computer Graphics Forum*, 2019. 2

[25] Martin Heusel, Hubert Ramsauer, Thomas Unterthiner, Bernhard Nessler, and Sepp Hochreiter. Gans trained by a two time-scale update rule converge to a local nash equilibrium. In *Advances in Neural Information Processing Systems (NIPS)*, 2017. 5

[26] Geoffrey E. Hinton and Ruslan Salakhutdinov. Reducing the dimensionality of data with neural networks. *Science*, 313:504–507, 2006. 2

[27] Binh-Son Hua, Minh-Khoi Tran, and Sai-Kit Yeung. Pointwise convolutional neural networks. In *Proc. IEEE Conf. on Computer Vision and Pattern Recognition (CVPR)*, 2018. 2

[28] Huaibo Huang, Zhihang Li, Ran He, Zhenan Sun, and Tieniu Tan. Introspective variational autoencoders for photographic image synthesis. In *Advances in Neural Information Processing Systems (NIPS)*, 2018. 2

[29] Phillip Isola, Jun-Yan Zhu, Tinghui Zhou, and Alexei A. Efros. Image-to-image translation with conditional adversarial networks. In *Proc. IEEE Conf. on Computer Vision and Pattern Recognition (CVPR)*, 2017. 2

[30] Wenzel Jakob. Mitsuba renderer, 2010. http://www.mitsuba-renderer.org. 5

[31] Krishna Murthy Jatavallabhula, Edward J. Smith, Jean-Francois Lafleche, Clement Fuji Tsang, Artem Rozantsev, Wenzheng Chen, Tommy Xiang, Rev Lebaredian, and Sanja Fidler. Kaolin: A pytorch library for accelerating 3d deep learning research. *arXiv.org*, 1911.05063, 2019. 2

[32] Henrik Wann Jensen. Global illumination using photon maps. In *Proceedings of the Eurographics Workshop on Rendering Techniques*, 1996. 3

[33] James T. Kajiya. The rendering equation. In *ACM Trans. on Graphics*, 1986. 1

[34] Tero Karras, Timo Aila, Samuli Laine, and Jaakko Lehtinen. Progressive growing of GANs for improved quality, stability, and variation. In *Proc. of the International Conf. on Learning Representations (ICLR)*, 2018. 1, 2

[35] Tero Karras, Samuli Laine, and Timo Aila. A style-based generator architecture for generative adversarial networks. In *Proc. IEEE Conf. on Computer Vision and Pattern Recognition (CVPR)*, 2019. 1, 2

[36] Hiroharu Kato, Yoshitaka Ushiku, and Tatsuya Harada. Neural 3d mesh renderer. In *Proc. IEEE Conf. on Computer Vision and Pattern Recognition (CVPR)*, 2018. 2

[37] Diederik P. Kingma and Jimmy Ba. Adam: A method for stochastic optimization. In *Proc. of the International Conf. on Learning Representations (ICLR)*, 2015. 5

[38] Diederik P. Kingma and Max Welling. Auto-encoding variational bayes. *Proc. of the International Conf. on Learning Representations (ICLR)*, 2014. 2

[39] Alexander Krull, Tim-Oliver Buchholz, and Florian Jug. Noise2void - learning denoising from single noisy images. In *Proc. IEEE Conf. on Computer Vision and Pattern Recognition (CVPR)*, 2019. 4

[40] Tejas D. Kulkarni, William F. Whitney, Pushmeet Kohli, and Joshua B. Tenenbaum. Deep convolutional inverse graphics network. In *Advances in Neural Information Processing Systems (NIPS)*, 2015. 2

[41] Eric P Lafortune and Yves D Willems. Bi-directional path tracing. 1993. 4

[42] Jaakko Lehtinen, Jacob Munkberg, Jon Hasselgren, Samuli Laine, Tero Karras, Miika Aittala, and Timo Aila. Noise2noise: Learning image restoration without clean data. In *Proc. of the International Conf. on Machine learning (ICML)*, 2018. 4, 5

[43] Tzu-Mao Li, Miika Aittala, Frédo Durand, and Jaakko Lehtinen. Differentiable monte carlo ray tracing through edge sampling. *ACM Trans. on Graphics*, 2018. 2

[44] Yiyi Liao, Katja Schwarz, Lars Mescheder, and Andreas Geiger. Towards unsupervised learning of generative models for 3d controllable image synthesis. In *Proc. IEEE Conf. on Computer Vision and Pattern Recognition (CVPR)*, 2020. 2

[45] Stephen Lombardi, Jason M. Saragih, Tomas Simon, and Yaser Sheikh. Deep appearance models for face rendering. *ACM Trans. on Graphics*, 37(4):68:1–68:13, 2018. 2

[46] Stephen Lombardi, Tomas Simon, Jason Saragih, Gabriel Schwartz, Andreas Lehrmann, and Yaser Sheikh. Neural volumes: Learning dynamic renderable volumes from images. In *ACM Trans. on Graphics*, 2019. 2

[47] Matthew M. Loper and Michael J. Black. Opendr: An approximate differentiable renderer. In *Proc. of the European Conf. on Computer Vision (ECCV)*, 2014. 2

[48] Michael Mara, Morgan McGuire, Benedikt Bitterli, and Wojciech Jarosz. An efficient denoising algorithm for global illumination. In *High-Performance Graphics (HPG)*, 2017. 2

[49] Ricardo Martin-Brualla, Noha Radwan, Mehdi S. M. Sajjadi, Jonathan T. Barron, Alexey Dosovitskiy, and Daniel Duckworth. Nerf in the wild: Neural radiance fields for unconstrained photo collections. *arXiv.org*, 2008.02268, 2020. 2

[50] Lars Mescheder, Andreas Geiger, and Sebastian Nowozin. Which training methods for gans do actually converge? In *Proc. of the International Conf. on Machine learning (ICML)*, 2018. 1, 2

[51] Lars Mescheder, Michael Oechsle, Michael Niemeyer, Sebastian Nowozin, and Andreas Geiger. Occupancy networks: Learning 3d reconstruction in function space. In *Proc. IEEE Conf. on Computer Vision and Pattern Recognition (CVPR)*, 2019. 2

[52] Moustafa Meshry, Dan B Goldman, Sameh Khamis, Hugues Hoppe, Rohit Pandey, Noah Snavely, and Ricardo Martin-Brualla. Neural rerendering in the wild. In *Proc. IEEE Conf. on Computer Vision and Pattern Recognition (CVPR)*, 2019. 1, 2

[53] Ben Mildenhall, Pratul P Srinivasan, Matthew Tancik, Jonathan T Barron, Ravi Ramamoorthi, and Ren Ng. NeRF: Representing scenes as neural radiance fields for view synthesis. In *Proc. of the European Conf. on Computer Vision (ECCV)*, 2020. 1, 2

[54] Thomas Müller, Brian Mcwilliams, Fabrice Rousselle, Markus Gross, and Jan Novák. Neural importance sampling. *ACM Trans. on Graphics*, 2019. 2

[55] Oliver Nalbach, Elena Arabadzhiyska, Dushyant Mehta, Hans-Peter Seidel, and Tobias Ritschel. Deep shading: Convolutional neural networks for screen space shading. *Computer Graphics Forum*, 36(4):65–78, 2017. 2

[56] Thu Nguyen-Phuoc, Chuan Li, Stephen Balaban, and Yong-Liang Yang. Rendernet: A deep convolutional network for differentiable rendering from 3d shapes. In *Advances in Neural Information Processing Systems (NIPS)*, 2018. 2

[57] Thu Nguyen-Phuoc, Chuan Li, Lucas Theis, Christian Richardt, and Yong-Liang Yang. Hologan: Unsupervised learning of 3d representations from natural images. In *Proc. of the IEEE International Conf. on Computer Vision (ICCV)*, 2019. 2

[58] Thu Nguyen-Phuoc, Christian Richardt, Long Mai, Yong-Liang Yang, and Niloy Mitra. Blockgan: Learning 3d

object-aware scene representations from unlabelled images. *arXiv.org*, 2020. 2

[59] Michael Niemeyer, Lars Mescheder, Michael Oechsle, and Andreas Geiger. Differentiable volumetric rendering: Learning implicit 3d representations without 3d supervision. In *Proc. IEEE Conf. on Computer Vision and Pattern Recognition (CVPR)*, 2020. 2

[60] Merlin Nimier-David, Delio Vicini, Tizian Zeltner, and Wenzel Jakob. Mitsuba 2: a retargetable forward and inverse renderer. 38(6):203, 2019. 2

[61] Atsuhiro Noguchi and Tatsuya Harada. RGBD-GAN: unsupervised 3d representation learning from natural image datasets via RGBD image synthesis. *arXiv.org*, 1909.12573, 2019. 1

[62] Michael Oechsle, Lars Mescheder, Michael Niemeyer, Thilo Strauss, and Andreas Geiger. Texture fields: Learning texture representations in function space. In *Proc. of the IEEE International Conf. on Computer Vision (ICCV)*, 2019. 2, 5

[63] Eunbyung Park, Jimei Yang, Ersin Yumer, Duygu Ceylan, and Alexander C. Berg. Transformation-grounded image generation network for novel 3d view synthesis. In *Proc. IEEE Conf. on Computer Vision and Pattern Recognition (CVPR)*, 2017. 2

[64] Matt Pharr, Wenzel Jakob, and Greg Humphreys. *Physically based rendering: From theory to implementation*. Morgan Kaufmann, 2016. 1, 2

[65] Francesco Pittaluga, Sanjeev J. Koppal, Sing Bing Kang, and Sudipta N. Sinha. Revealing scenes by inverting structure from motion reconstructions. In *Proc. IEEE Conf. on Computer Vision and Pattern Recognition (CVPR)*, 2019. 2

[66] Charles R Qi, Hao Su, Kaichun Mo, and Leonidas J Guibas. Pointnet: Deep learning on point sets for 3d classification and segmentation. In *Proc. IEEE Conf. on Computer Vision and Pattern Recognition (CVPR)*, 2017. 1, 3, 5

[67] Charles R Qi, Li Yi, Hao Su, and Leonidas J Guibas. Pointnet++: Deep hierarchical feature learning on point sets in a metric space. In *Advances in Neural Information Processing Systems (NIPS)*, 2017. 2

[68] Gilles Rainer, Wenzel Jakob, Abhijeet Ghosh, and Tim Weyrich. Neural btf compression and interpolation. *Computer Graphics Forum*, 2019. 2

[69] Konstantinos Rematas and Vittorio Ferrari. Neural voxel renderer: Learning an accurate and controllable rendering tool. In *Proc. IEEE Conf. on Computer Vision and Pattern Recognition (CVPR)*, 2020. 2

[70] Peiran Ren, Jiaping Wang, Minmin Gong, Stephen Lin, Xin Tong, and Baining Guo. Global illumination with radiance regression functions. *ACM Trans. on Graphics*, 2013. 2

[71] Helge Rhodin, Mathieu Salzmann, and Pascal Fua. Unsupervised geometry-aware representation for 3d human pose estimation. In *Proc. of the European Conf. on Computer Vision (ECCV)*, 2018. 2

[72] Gernot Riegler and Vladlen Koltun. Free view synthesis. In *Proc. of the European Conf. on Computer Vision (ECCV)*, 2020. 2

[73] Olaf Ronneberger, Philipp Fischer, and Thomas Brox. U-net: Convolutional networks for biomedical image segmentation. In *Medical Image Computing and Computer-Assisted Intervention (MICCAI)*, 2015. 4, 5

[74] Christoph Schied, Anton Kaplanyan, Chris Wyman, Anjul Patney, Chakravarty R. Alla Chaitanya, John Burgess, Shiqiu Liu, Carsten Dachsbacher, Aaron E. Lefohn, and Marco Salvi. Spatiotemporal variance-guided filtering: real-time reconstruction for path-traced global illumination. In *High-Performance Graphics (HPG)*, 2017. 2

[75] Christoph Schied, Christoph Peters, and Carsten Dachsbacher. Gradient estimation for real-time adaptive temporal filtering. *PACMCGIT*, 2018. 2

[76] Katja Schwarz, Yiyi Liao, Michael Niemeyer, and Andreas Geiger. Graf: Generative radiance fields for 3d-aware image synthesis. In *Advances in Neural Information Processing Systems (NeurIPS)*, 2020. 2

[77] Ashish Shrivastava, Tomas Pfister, Oncel Tuzel, Joshua Susskind, Wenda Wang, and Russell Webb. Learning from simulated and unsupervised images through adversarial training. In *Proc. IEEE Conf. on Computer Vision and Pattern Recognition (CVPR)*, 2017. 1

[78] Vincent Sitzmann, Justus Thies, Felix Heide, Matthias Nießner, Gordon Wetzstein, and Michael Zollhöfer. Deepvoxels: Learning persistent 3d feature embeddings. In *Proc. IEEE Conf. on Computer Vision and Pattern Recognition (CVPR)*, 2019. 1, 2

[79] Vincent Sitzmann, Michael Zollhöfer, and Gordon Wetzstein. Scene representation networks: Continuous 3d-structure-aware neural scene representations. In *Advances in Neural Information Processing Systems (NIPS)*, 2019. 2

[80] Christian Szegedy, Wei Liu, Yangqing Jia, Pierre Sermanet, Scott E. Reed, Dragomir Anguelov, Dumitru Erhan, Vincent Vanhoucke, and Andrew Rabinovich. Going deeper with convolutions. In *Proc. IEEE Conf. on Computer Vision and Pattern Recognition (CVPR)*, 2015. 5

[81] Christian Szegedy, Vincent Vanhoucke, Sergey Ioffe, Jonathon Shlens, and Zbigniew Wojna. Rethinking the inception architecture for computer vision. In *Proc. IEEE Conf. on Computer Vision and Pattern Recognition (CVPR)*, 2016. 5

[82] Maxim Tatarchenko, Alexey Dosovitskiy, and Thomas Brox. Multi-view 3d models from single images with a convolutional network. In *Proc. of the European Conf. on Computer Vision (ECCV)*, 2016. 2

[83] Justus Thies, Michael Zollhöfer, and Matthias Nießner. Deferred neural rendering: image synthesis using neural textures. In *ACM Trans. on Graphics*, 2019. 2

[84] Julien Valentin, Cem Keskin, Pavel Pidlypenskyi, Ameesh Makadia, Avneesh Sud, and Sofien Bouaziz. Tensorflow graphics: Computer graphics meets deep learning. 2019. 2

[85] Gül Varol, Javier Romero, Xavier Martin, Naureen Mahmood, Michael J. Black, Ivan Laptev, and Cordelia Schmid. Learning from synthetic humans. In *Proc. IEEE Conf. on Computer Vision and Pattern Recognition (CVPR)*, 2017. 1

[86] Eric Veach. *Robust Monte Carlo Methods for Light Transport Simulation*. PhD thesis, Stanford University, Stanford, CA, USA, 1998. 1, 2, 5

[87] Delio Vicini, Vladlen Koltun, and Wenzel Jakob. A learned shape-adaptive subsurface scattering model. *ACM Trans. on Graphics*, 2019. 2

[88] Ting-Chun Wang, Ming-Yu Liu, Jun-Yan Zhu, Andrew Tao, Jan Kautz, and Bryan Catanzaro. High-resolution image synthesis and semantic manipulation with conditional gans. In *Proc. IEEE Conf. on Computer Vision and Pattern Recognition (CVPR)*, 2018. 2

[89] Zhou Wang, Alan C. Bovik, Hamid R. Sheikh, and Eero P. Simoncelli. Image quality assessment: from error visibility to structural similarity. *IEEE Trans. on Image Processing (TIP)*, 13(4):600–612, 2004. 5

[90] Daniel E. Worrall, Stephan J. Garbin, Daniyar Turmukhambetov, and Gabriel J. Brostow. Interpretable transformations with encoder-decoder networks. In *Proc. of the IEEE International Conf. on Computer Vision (ICCV)*, 2017. 2

[91] Xinchen Yan, Jimei Yang, Ersin Yumer, Yijie Guo, and Honglak Lee. Perspective transformer nets: Learning single-view 3d object reconstruction without 3d supervision. In *Advances in Neural Information Processing Systems (NIPS)*, 2016. 2

[92] Xiuming Zhang, Sean Ryan Fanello, Yun-Ta Tsai, Tiancheng Sun, Tianfan Xue, Rohit Pandey, Sergio Orts-Escolano, Philip L. Davidson, Christoph Rhemann, Paul E. Debevec, Jonathan T. Barron, Ravi Ramamoorthi, and William T. Freeman. Neural light transport for relighting and view synthesis. *arXiv.org*, 2008.03806, 2020. 2

[93] Zhiyuan Zhang, Binh-Son Hua, and Sai-Kit Yeung. Shellnet: Efficient point cloud convolutional neural networks using concentric shells statistics. In *Proc. of the IEEE International Conf. on Computer Vision (ICCV)*, 2019. 2

[94] Tinghui Zhou, Shubham Tulsiani, Weilun Sun, Jitendra Malik, and Alexei A. Efros. View synthesis by appearance flow. In *Proc. of the European Conf. on Computer Vision (ECCV)*, 2016. 2